sustainability

MDPI

Article

Evaluation and Comparison of TRMM Multi-Satellite Precipitation Products With Reference to Rain Gauge Observations in Hunza River Basin, Karakoram Range, Northern Pakistan

Ayaz Fateh Ali [1,2,*], Cunde Xiao [1,2,3], Muhammad Naveed Anjum [1,2], Muhammad Adnan [1,2], Zain Nawaz [2,4], Muhammad Wajid Ijaz [5], Muhammad Sajid [6] and Hafiz Umar Farid [7]

1 State Key Laboratory of Cryospheric Science, Northwest Institute of Eco-Environment and Resources, Chinese Academy of Sciences, Lanzhou 730000, China; cdxiao@lzb.ac.cn (C.X.); naveedwre@lzb.ac.cn (M.N.A.); adnan@lzb.ac.cn (M.A.)
2 University of Chinese Academy of Sciences, Beijing 100049, China; zain-nawaz@lzb.ac.cn
3 State Key Laboratory of Land Surface and Resource Ecology, Beijing Normal University, Beijing 100875, China
4 Laboratory of Remote Sensing and Information Resources for Cold and Arid Regions, Northwest Institute of Eco-Environment and Resources, Chinese Academy of Sciences, Lanzhou 730000, China
5 United States-Pakistan Centre for Advanced Studies in Water, Mehran University of Engineering and Technology, Jamshoro, 76062 Sindh, Pakistan; wajidijaz331@gmail.com
6 Department of Zoology, Government College University Faisalabad, Allama Iqbal Road, Faisalabad 38000, Pakistan; naveedwre@yahoo.com
7 Department of Agricultural Engineering, Faculty of Agricultural Sciences and Technology, Bahauddin Zakariya University, Multan 60800, Pakistan; farid_vjr@yahoo.com
* Correspondence: ayaz@lzb.ac.cn; Tel.: +86-186-0944-7913

Received: 22 August 2017; Accepted: 24 October 2017; Published: 31 October 2017

Abstract: The performance evaluation of satellite-based precipitation products at local and regional scales is crucial for modification in satellite-based precipitation retrieval algorithms, as well as for the provision of guidance during the selection of substitute precipitation data. This study evaluated the performances of three Tropical Rainfall Measuring Mission (TRMM) Multi-satellite Precipitation Analysis (TMPA) products (3B42V6, 3B42RT and 3B42V7) with a reference to rain gauge observations in the Hunza River basin, northern Pakistan. Multi-spatial (pixel and basin) and temporal (daily, monthly, seasonal and annual) resolutions were considered for performance evaluation of TMPA products. Results revealed that the spatial pattern of observed precipitation over the basin was adequately captured by 3B42V7 but misplaced by 3B42V6 and 3B42RT. All TMPA products were unable to capture the intense precipitation events. On the daily time scale, the performance of TMPA products was very poor over both spatial scales. 3B42V6 underestimated the precipitation (31.25% and 44.27% on pixel and basin scales, respectively). By contrast, 3B42RT significantly overestimated the precipitation (47.91% and 38.62% on pixel and basin scales, respectively), while 3B42V7 showed overestimation (17.30%) on pixel scale and slight underestimation (6.24%) on the basin scale. On the seasonal scale, TMPA products showed significant biases with observed precipitation data. We found that the TMPA products performed relatively better on monthly and annual time scales and overall performance of 3B42V7 product was better than that of 3B42V6 and 3B42RT. The bias in 3B42V7 was improved by 85.90% compared with 3B42V6 and by 116.16% compared with 3B42RT. Thus, it is concluded that the TMPA products were unreliable to capture the intense precipitation events and retain high errors on daily and seasonal scales. Therefore, caution should be considered while using these precipitation estimates as a substitute data in hydrology, meteorology and climatology studies in Hunza River basin. However, due to the reasonable performance of monthly and annual 3B42V7 estimates, these can be used as an acceptable substitute for applications in the region.

Keywords: Hunza River basin; Karakoram Range; satellite precipitation; evaluation

1. Introduction

Precipitation is an important parameter of the hydrological cycle and is one of the main sources of water supplies for agriculture, humans, and wildlife to sustain life. Acquiring precise precipitation information is thus crucial for sustainable management of water resources. However, precipitation observations are generally limited to ground-based measurements, and, usually, these ground-based records have low spatial and/or temporal coverages, especially in physically inaccessible river basins such as ones nested in the Hindukush–Karakoram–Himalayan (HKH) region.

At present, development of remote sensing has provided plenty of resources for understanding the spatio-temporal variability in precipitation, particularly in high altitude regions where ground-based observations are not readily available or very scarce [1–3]. To date, several high-resolution satellite-based precipitation products have been operationally available to provide the precipitation information for different hydro-climatological applications. Among these precipitation products, the Tropical Rainfall Measuring Mission (TRMM) Multi-satellite Precipitation Analysis (TMPA) products developed by the National Aeronautics and Space Administration (NASA and the Japanese Aerospace Exploration Agency (JAXA), are widely used to monitor the precipitation over tropical and subtropical regions. This mission has been functioning since November 1997 and releasing precipitation products since 1998. The TRMM covers regions (over latitude 50° N to 50° S) at fine spatiotemporal resolutions (0.25° × 0.25° and 3 hourly) [2]. TMPA products are available for near real time (3B42RT) and post real time (3B42V6 and 3B42V7) precipitation events. The precipitation retrieval algorithms for the post real time products (3B42V6 and 3B42V7) combine a number of ground-based precipitation observations with microwave (MW) and infrared (IR) precipitation estimates. The MW estimates are derived from several sensors including TRMM MW imager (TMI), Advanced MW Sounding Unit-B (AMSU-B), Advanced MW Scanning Radiometer-Earth Observing System (AMSR-E), and the Spectral Sensor MW Imager (SSMI, only for 3B42V7 estimates). IR estimates used in TMPA algorithms are acquired from Geosynchronous Earth Orbit (GEO) IR sensors. The combined estimates from MW and IR sensors are used to generate real time precipitation product (3B42RT). The post real time products (3B42V6 and 3B42V7) are then generated by combining 3B42RT estimates with the precipitation estimates from the Climate Assessment and Monitoring System (CAMS, only for 3B42V6 product), Global Precipitation Climatology Center (GPCC), TRMM Precipitation Radar, and TMI [4].

Since the launch of TRMM mission, it has undergone several major enhancements by incorporating additional sensors and upgraded algorithms. The 3B42V6 product was launched in 2009 after incorporating the climatological calibration algorithm (CCA) for reduction of bias in TMPA V5 (not included in this analysis) algorithm. After substantial changes in the algorithm of 3B42V6, it was replaced with an updated version of TMPA products (3B42V7) in June 2012. The upgraded algorithm used in 3B42V7 combines the estimates from the MW Humidity Sounder (MWHS), TRMM Precipitation Radar (TPR), SSMI, GPCC, and National Climatic Data Centre (NCDC). After the success of TRMM project, NASA and JAXA launched a successor to TMPA products in early 2014, known as GPM product (not included in this study), by combining the algorithm of upgraded TMPA product with Climate Prediction Centre Morphing technique (CMORPH) and Precipitation Estimation from the Remotely Sensed Information Using Artificial Network (PERSIANN) [5]. Therefore, comprehensive assessments and comparisons of the performance of the upgraded TMPA algorithm relative to its predecessor and real time versions in different regions, precipitation patterns and topographic conditions would be valuable for algorithm developers, particularly for GPM, as well as satellite-based precipitation data users.

It is well reported that the accuracy of satellite-based precipitation products is dependent on precipitation variability, topography, and climate [6–10]. A large number of studies have evaluated the performance of 3V42V6 in many parts of world [11–15]. Although some studies have also documented the performance of 3B42V7 in different regions of the world [14–18], limited studies have reported on its performance relative to its predecessor (3B42V6) and near real time product (3B42RT) in complex terrain regions having cryospheric environment. Thus, a river basin situated in the high mountains of Hindukush– Karakoram–Himalayan (HKH) region [15,19] has been chosen for undertaking a comprehensive and comparative assessment of TMPA products with a wide variety of statistical indicators.

A number of researchers have evaluated the performance of satellite-based precipitation products with reference to in-situ rain gauge observations on pixel and basin scales in different regions of the world and reported that the performance of satellite-based precipitation products varies from area to area because of different topographic and atmospheric conditions [20–22]. Among them, Liu et al. [23] reported that the in-situ and pixel scale knowledge of precipitation is essential for meteorological studies, but large-scale (basin level) precipitation information is very important for hydrological and climatological applications. However, on basin scale, there is a possibility of stochastic errors and bias in precipitation retrieval from the satellite-based precipitation products due to complex topography and related orographic lifting processes or inadequate sensitivity of the satellite sensors in snow-dominated regions. Despite the fact that the basin-wide performance evaluation of satellite-based precipitation products, particularly in snow-dominated regions, is necessary to the users and algorithm developers for understanding the uncertainties associated with the satellite-based precipitation retrieval algorithms, the precision of these products in such areas on basin-scale is often unreported in most of the existing evaluation studies [24]. Therefore, comprehensive evaluations of the satellite precipitation products are still crucial for better understanding of their performances in different topographic regions, spatio-temporal scales, and precipitation patterns. Thus far, the performances of TMPA precipitation products are usually undocumented at different spatio-temporal scales particularly in complex terrain and snow dominated river basins. Therefore, the performance of these satellite-based precipitation products need be evaluated at different time periods in such areas to enable researchers and algorithm developers to quantify and overcome the uncertainties.

Thus, the present study was conducted to focus on two aspects. First, to evaluate the accuracy of most widely used global high-resolution TMPA satellite precipitation products (3B42V6, 3B42RT and 3B42V7) with reference to rain gauge observations on different spatio-temporal scales over the Hunza Basin in Karakoram Mountainous range, northern Pakistan. Second, to assess the performance improvements of the upgraded 3B42V7 algorithm compared with 3B42V6 and 3B42RT. The present article is organized as follows: Section 2 describes the study area, datasets used, and detailed methodology; Section 3 presents the results and discussions; and conclusions of this study are given in Section 4.

2. Study Area, Datasets, and Methodology

2.1. Study Area

The Hunza River basin, a tributary of the Upper Indus basin with a total drainage area of 13,733 km^2, is located in the northern Pakistan (Figure 1). The Hunza Basin is situated at the junction of two high mountains Karakoram and Hindukush in the proximity of China–Pakistan border. This basin has a complex topography, with elevation ranging from 1420 m above sea level (m.a.s.l.) (southern part) to 7809 m a.s.l. (northern part). The mean annual precipitation varies from 170 mm in the northeast to 680 mm in the southwest periphery of the basin. This is a snow-dominated river basin [25] and lies in the monsoon (July to September) and westerlies (January to March) belt.

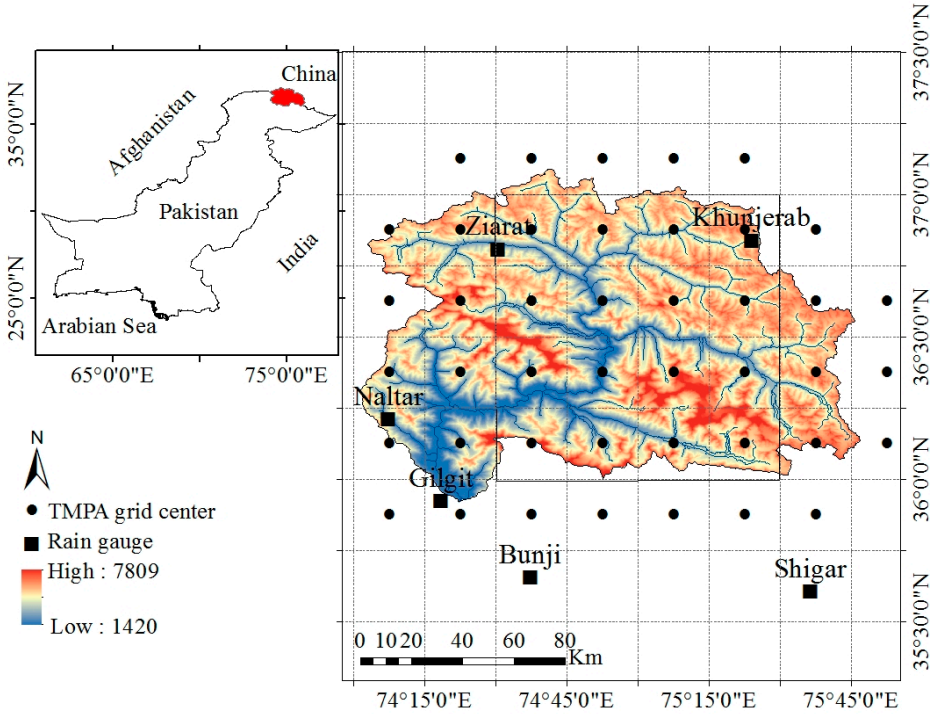

Figure 1. Location map of Hunza Basin in Pakistan, its elevation and location of rain gauges.

2.2. Datasets

The observed hourly-based precipitation records of the eight rain gauge stations located within and neighboring the Hunza Basin were obtained from Water and Power Development Authority of Pakistan (WAPDA) and Pakistan Meteorological Department (PMD). Because this is a snow-dominated basin, winter precipitation was recorded in terms of water equivalent, which was obtained by melting the snow or ice with hot water in the standard vessel and then removing the volume of hot water from the total volume. Precipitation records of only six stations were selected (for the period of 10 years covering 1999–2008) based on data quality and continuity of the data. We followed the World Meteorological Organization (WMO) standard code WMO-N for collection, analyses, and correction of gauge-based precipitation data [26]. Therefore, precipitation data of the selected stations were considered as ground truth for evaluation of satellite-based precipitation products. Key features of selected rain gauging stations are presented in Table 1.

Table 1. Key features of automatic rain gauge stations used in this study.

No.	Station	Elevation (m)	Latitude	Longitude	Average Annual Precipitation (mm)
1	Bunji	1372	35°40′04″ N	74°38′01″ E	147
2	Gilgit	1479	35°55′34″ N	74°22′16″ E	137
3	Khunjrab	4440	35°50′28″ N	75°25′09″ E	176
4	Naltar	2898	36°10′00″ N	74°11′00″ E	684
5	Shigar	2367	35°38′00″ N	75°32′00″ E	400
6	Ziarat	3020	36°13′00″ N	74°26′00″ E	235

We used near real time (3B42RT) and post real time (3B42V6 and 3B42V7) TMPA precipitation products for the performance evaluation and comparison. The 3B42RT product was evaluated over the period of nine years (2000–2008), while 3B42V6 and 3B42V7 were evaluated over the period of 10 years (1999–2008). These fine scale (3 hourly and 0.25° × 0.25°) satellite precipitation products are freely available on a global belt of 50° N–50° S and can be found at TRMM website (http://disc2.nascom.nasa.gov/tovas/). Detailed information about processing algorithm of 3B42V6 can be found

in [2] while changes made in the processing algorithm of latest version 7 (3B42V7) of TMPA products are described in [27]. A brief description of 3B42RT product is presented in [28]. The daily, monthly, seasonal, and annual precipitation estimates of TMPA products were obtained by aggregating the three-hourly estimates. To evaluate the performances of TMPA products on grid/pixel scale, more than one gauging station is required within the same grid (0.25° × 0.25°) or pixel (1° × 1°) [1]. In the present study area, the gauging stations are sparse and unevenly distributed and no TMPA grid contains more than one rain gauge stations. However, more than one gauging stations were available on pixel (1° × 1°) scale. Co-kriging approach was used to estimate the gauge-based areal average precipitation over the pixel and basin scales to solve the scale discrepancy and to compare the gauge and satellite data on the same spatial scales. To estimate the satellite-based areal average precipitation estimates the values of all the TMPA grids that lie within the pixel/basin boundary were averaged.

2.3. Methods for Accuracy Assessment

The accuracies of TMPA products were investigated on the pixel (1° × 1°) and basin scales. For both spatial scales, performances were evaluated on four temporal scales i.e., daily, monthly, seasonal and annual. In case of seasonal analysis, we evaluated and compared the performances of TMPA products in main rainy seasons (i.e., monsoon and westerlies) of this region. Considering the topography and sparse rain gauge stations, we adopted a geostatistical approach, co-kriging for estimation of areal average gauge-based precipitation. A detailed description and procedure of co-kriging are presented in [29,30]. Several statistical indices (continuous evaluation indices and categorical indices) were adhered for investigation of accuracy (of TMPA precipitation products) in terms of consistency and discrepancy [25,31]. Consistency shows the propinquity or similarity between rain gauge and TMPA-based precipitation estimates, whereas the discrepancy refers to the difference or the ratio between the observed (gauge-based) and estimated (satellite-based) precipitation estimates [32].

2.3.1. Continuous Evaluation Indices

The performances of TMPA products were evaluated by using several widely used continuous evaluation indices (equations are given in Appendix A). Among them, the slope coefficient of linear regression was used to assess the consistency between satellite-based and observed precipitation estimates. Pearson's correlation coefficient (r) is a statistical index which gives the degree of linear association between satellite precipitation and gauge observations. The discrepancy between the satellite and gauge precipitation data was quantified by mean error (ME), mean absolute error (MAE), the root mean square error (RMSE), normalized root mean square error (NRMSE) and normalized mean absolute error (NMAE).

The error (E) and relative error (RE) were computed to quantify the individual errors. The E describes the difference between the satellite precipitation estimates and gauge observations (i.e., E is a measure of how far a satellite estimate is from gauge observation), whereas RE measures how large the error is compared with gauge observation. The average discrepancy between the satellite precipitation and gauge observations was estimated by mean error (ME), while the mean absolute error (MAE) was used the measure the average magnitude of the error. The bias describes the scale of the overall deviation of satellite estimates from rain gauge observations (i.e., the degree of over or underestimation of precipitation). The root mean square error (RMSE) was estimated to scale the average difference between the satellite precipitation and rain gauge observations. The normalized root mean square error (NRMSE) and normalized mean absolute error (NMAE) were computed to assess the reliability of the estimates.

2.3.2. Categorical Indices

For more precise quantification of errors in the 3B42V6, 3B42RT and 3B42V7 products, three additional categorical statistical indices, (probability of detection (POD), false alarm

ratio (FAR), and critical success index (CSI)) were used to detect the agreement between the gauged-based and TMPA-based precipitation data at rain gauge locations (formulas are given in Appendix A). POD illustrates how often the precipitation events are appropriately sensed by satellites. FAR represents the fraction of precipitation events in which satellite detects the false occurrence of precipitation events. CSI represents the overall fraction of precipitation events when gauge-based observations were correctly predicted by satellite. Occurrence or absence of precipitation events was recognized by different thresholds. The perfect value of FAR is 0, while that for POD and CSI is 1.

3. Results and Discussions

3.1. Comparison of Spatial Patterns of TMPA and Gauge-Based Precipitation

Figure 2 illustrates the spatial patterns (Kriging interpolation technique was used) of average annual gauge-based (Figure 2a) and TMPA-based precipitation (Figure 2b–d) over the study area. The interpolated pattern of average annual gauge-based precipitation showed an increasing trend from northeast to the southwest direction of the basin. Despite the fact that 3V42V7 underestimated the precipitation magnitudes (Figure 2b), particularly in the southwestern part of the basin, it generally tried to capture the spatial pattern of the observed precipitation over the study area. 3B42V6 and 3B42RT products were totally failed to capture the spatial patterns and magnitudes of precipitation in this area (Figure 2c,d, respectively). A higher average annual precipitation pattern was detected in the central part of the basin by the 3B42RT, while 3B42V6 exhibited the higher average annual precipitation over the southern slopes of the basin. 3B42V6 and 3B42RT showed significant under and overestimations, respectively. This analysis revealed that the 3B42V6 and 3B42RT products were unsuitable to detect the spatial patterns of precipitation in northern Pakistan.

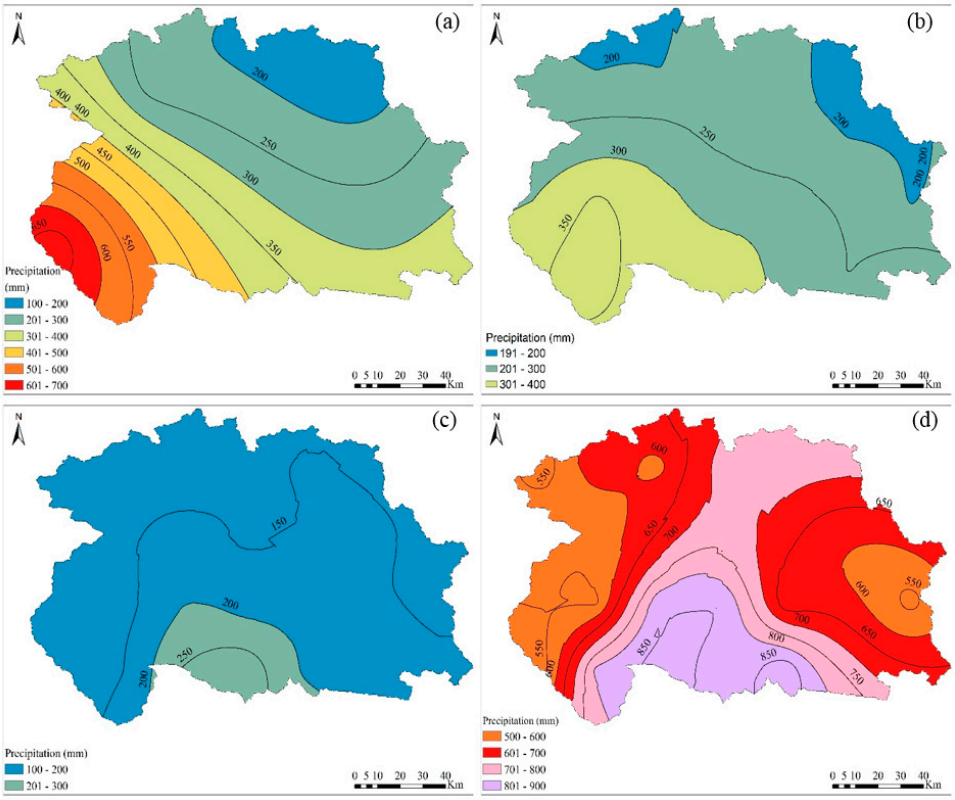

Figure 2. Spatial pattern of average annual precipitation: (**a**) gauge; (**b**) 3B42V7; (**c**) 3B42V6; and (**d**) 3B42RT.

3.2. Evaluation of TMPA Products at Different Spatial and Temporal Scales

The comparisons of daily TMPA (3B42V6, 3B42V7 and 3B42RT) precipitation estimates with rain gauge observations at pixel ($1^\circ \times 1^\circ$) and basin scales are shown in Figure 3. The daily precipitation estimates of TMPA products exhibited very poor agreement with the observed precipitation at both pixel and basin scales as witnessed by low values of r (0.20, 0.27 and 0.23 for 3B42V6, 3B42V7 and 3B42RT, respectively, on pixel scale and 0.34, 0.43 and 0.33 for 3B42V6, 3B42V7 and 3B42RT, respectively, on basin scale). The scores of linear regression coefficients (a = 0.20, 0.34 and 0.46 for 3B42V6, 3B42V7 and 3B42RT, respectively, on pixel scale (Figure 3a,c,e) and 0.32, 0.53 and 0.64 for 3B42V6, 3B42V7 and 3B42RT, respectively, on basin scale (Figure 3b,d,f)) also justified the poor performance of all TMPA-based precipitation products compared with the rain gauge data at both spatial scales. 3B42V6 showed significant underestimations of precipitation on both pixel (BIAS = −31.25%) and basin (BIAS = −44.27%) scales, while 3B42V7 slightly underestimated the precipitation on basin (BIAS = −6.24%) and overestimated on pixel (BAIS = 17.31%) scale. On the other hand, 3B42RT significantly overestimated the precipitation on both pixel and basin scales (47.91% and 38.62%, respectively). On pixel scale, 3B42V6, 3B42V7 and 3B42RT have ME values of −0.36 mm/day, 0.10 mm/day and 0.34 mm/day, respectively, while on basin scale the values of ME were −0.18 mm/day, −0.06 mm/day and 0.28 mm/day, respectively. The scores of other respective discrepancies were 0.70 mm/day (120%), 0.80 mm/day (140%) and 1.17 mm/day (164%) for MAE (NMAE) on pixel scale, whereas 0.69 mm/day (99%), 0.79 (106%) and 1.09 mm/day (152%) on basin scale. The scores of RMSE (NRMSE) were 1.60 mm/day (278%), 1.94 mm /day (313%) and 2.54 mm/day (354%) on pixel scale and 1.50 mm/day (203%), 1.53 mm/day (212%), and 2.36 mm/day (330%) on basin scale. Despite that the performance of TMPA products was slightly better on basin scale compared with the pixel scale, the high scores of errors indicated that the TMPA precipitation products (3B42V6, 3B42V7 and 3B42RT) are unsuitable to be used on the daily scale in the Karakoram Region.

The relationships between monthly total gauge-based and TMPA-based (3B42V6, 3B42V7 and 3B42RT) precipitation estimates on pixel and basin scales are shown in Figure 4. The TMPA products showed low agreements with rain gauge observations (r = 0.26, 0.33 and 0.14 for 3B42V6, 3B42V7 and 3B42RT, respectively) at pixel scale, whereas moderate agreements at basin scale (r = 0.52, 0.58 and 0.32 for 3B42V6, 3B42V7 and 3B42RT, respectively). It was found that, similar to daily time scale, the monthly TMPA-based estimates also have less agreement with the gauge-based precipitation data on pixel scale, as demonstrated by low values of r and liner regression coefficients (a = 0.19, 0.43 and 0.04 for 3B42V6, 3B42V7 and 3B42RT, respectively). The respective scores of all other discrepancies on the monthly time scale are the following: ME = −9.8 mm/month, 3.2 mm/month and 9.24 mm/month; MAE (NMAE) = 12.12 mm/month (56.13%), 11.14 mm/month (62.26%) and 16.44 mm/month (75.32%); RMSE (NRMSE) = 16.11 mm/month (76.42%), 15.63 mm/month (85.21%) and 24.85 mm/month (113.87%) were high compared with those on the basin scale (ME = −6.12 mm/month, −1.66 mm/month and 7.45 mm/month; MAE (NMAE) = 10.15 mm/month (51.90%), 9.91 mm/month (46.72%) and 14.78 mm/month (67.73%); and RMSE (NRMSE) = 14.61 mm/month (66.13%), 14.65 mm/month (62.71%) and 21.65 mm/month (99.19%). Results indicated that the accuracy was higher on basin scale compared with pixel scale and overall performance of monthly 3B42V7 estimates was better than that of monthly 3B42V6 and 3B42RT data. These findings are consistent with previous literature [14,18].

The comparison of 3B42V6 and 3B42RT on the annual scale also demonstrated the poor relationships of these products with gauge-based data on both spatial (pixel and basin) scales. Table 2 shows the annual evaluation results. The values of R were low (0.20 and 0.24 on pixel and 0.32 and 0.46 on basin scale for 3B42V6 and 3B42RT, respectively). Moreover, scores of all statistical errors were high (Table 2). Annual precipitation estimates of 3B42V7 product also exhibited poor relationship (r = 0.46) with gauge observations on pixel scale, but a good agreement (r = 0.72) between these two datasets was found on the basin scale (Table 2).

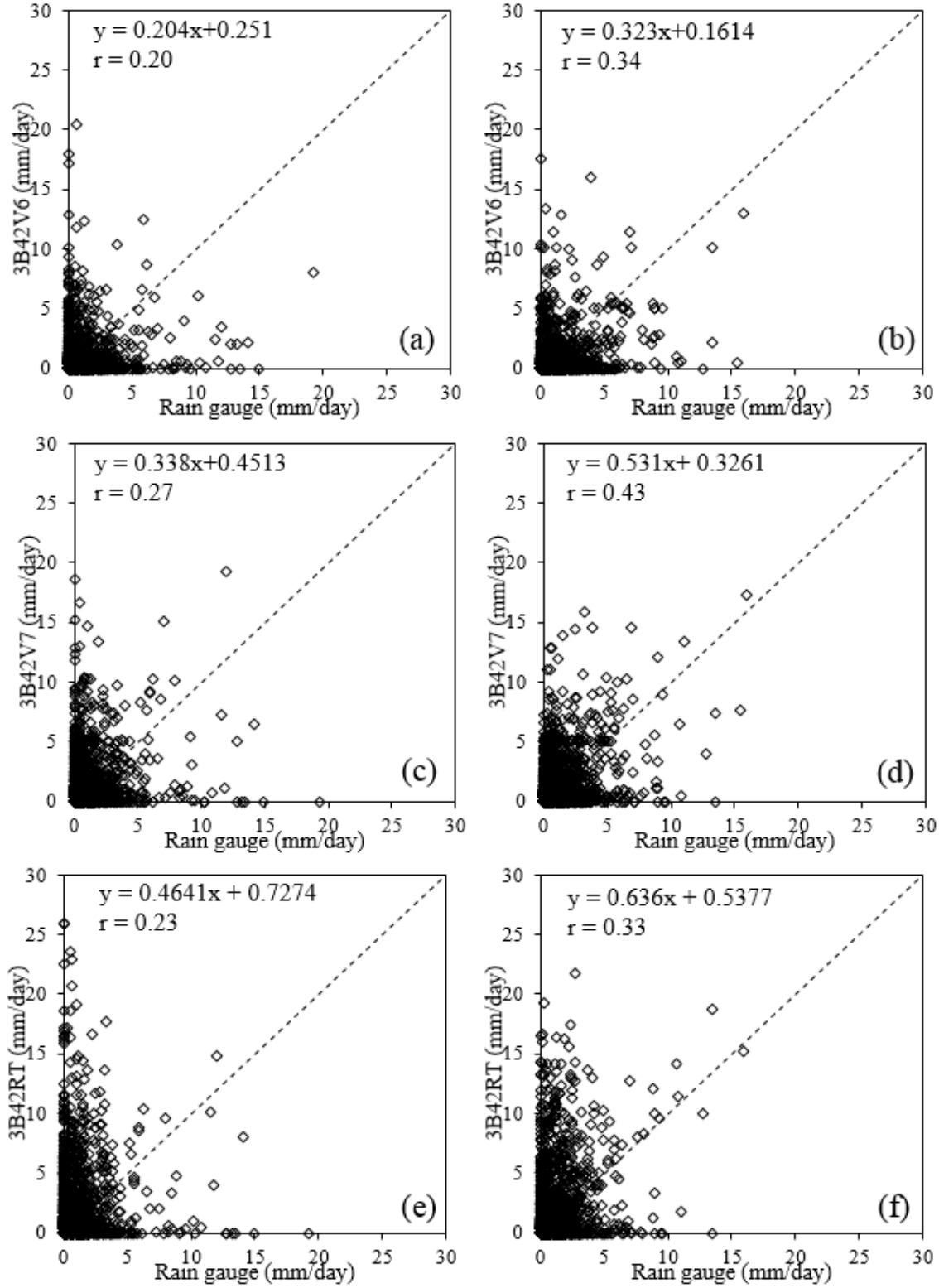

Figure 3. Scatter plots of daily satellite-based precipitation products: 3B42V6 (**a**,**b**); 3B42V7 (**c**,**d**); and 3B42RT (**e**,**f**) versus daily rain gauge observations at: 1° × 1° pixel (**a**,**c**,**e**); and basin (**b**,**d**,**f**) scales.

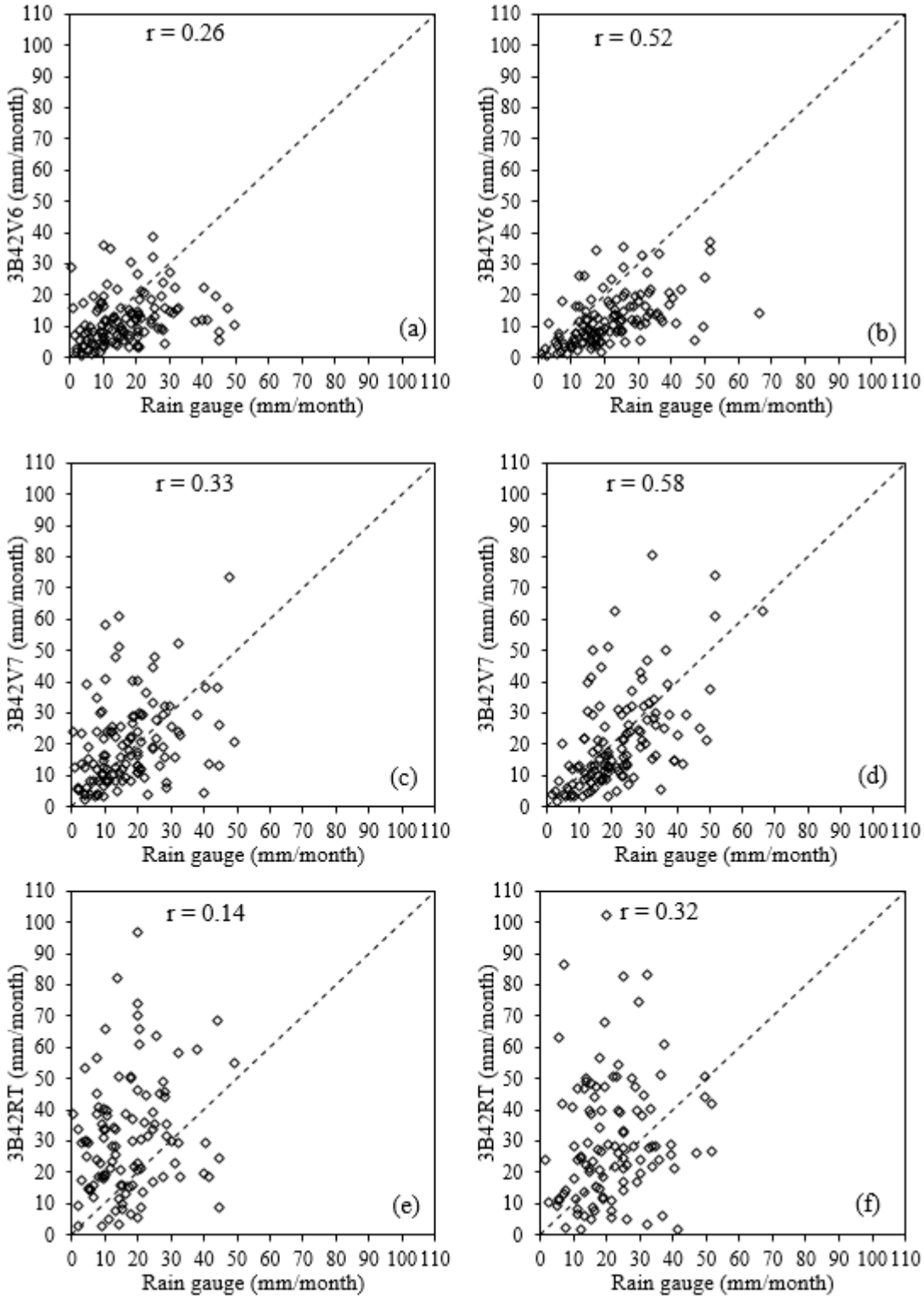

Figure 4. Scatter plots of monthly: 3B42V6 (**a**,**b**); 3B42V7 (**c**,**d**); and 3B42RT (**e**,**f**) estimates versus rain gauge observations at: pixel (**a**,**c**,**e**); and basin (**b**,**d**,**f**) scales.

Figure 5 illustrates the comparison of 3B42V6, 3B42V7 and 3B42RT performances on different spatial and temporal scales. Generally, 3B42V7 exhibited higher agreements with gauge observations as compared with 3B42V6 and 3B42RT. The values of R were higher for the basin scale compared with the pixel scale on all temporal (daily, monthly and annual) scales. The errors were higher in 3B42RT

estimates as compared to 3B42V6 and 3B42V7, as witnessed by higher values of NRMSE. Generally, NRMSE decreased with increasing spatio-temporal scales. Results for NMAS were same as that of NRMSE on all spatio-temporal scales.

Table 2. Statistical error characteristics of TMPA products at the annual scale.

Product	3B42V6		3B42V7		3B42RT	
	Pixel	Basin	Pixel	Basin	Pixel	Basin
r	0.20	0.32	0.46	0.72	0.24	0.46
ME	−65.14	−114.44	34.18	−14.20	158.71	87.31
MAE	66.12	114.44	66.91	65.35	163.32	97.72
NMAE	32.17	44.16	34.45	25.45	80.11	37.68
RMSE	84.78	123.10	88.07	78.74	199.36	117.07
NRMSE	41.68	47.71	42.44	30.50	97.79	45.14
BIAS	−31.25	−44.27	17.31	−6.24	47.91	38.62

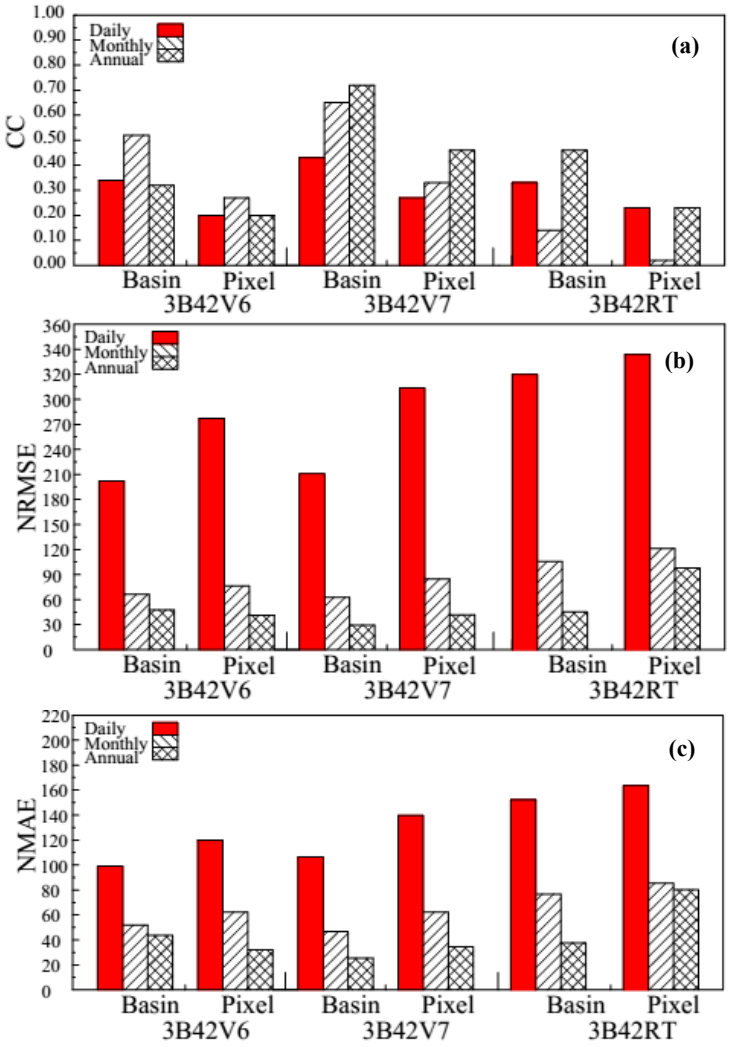

Figure 5. Comparison of validation indices for 3B42V6, 3B42V7 and 3B42RT on pixel and basin scales for: (**a**) correlation coefficient (CC); (**b**) normalized root mean square error (NRMSE); and (**c**) normalized mean absolute error (NMAE).

To evaluate the performance of TMPA products during rainy seasons, the errors in 3B42V6, 3B42RT and 3B42V7 were quantified and compared on different spatial (pixel and basin) scales during monsoon and westerlies. Findings revealed that TMPA products were less accurate during both seasons on both spatial scales. During westerlies, 3B42V6 overestimated (29.14%) the precipitation on pixel scale while underestimated it (−20.18%) on basin scale. 3B42V7 overestimated the precipitation on both spatial (pixel and basin) scales (67.78% and 24.28%, respectively). Precipitation magnitudes were significantly overestimated by 3B42RT on both spatial scales (54.03% and 54.88% on pixel and basin scales, respectively). During the monsoon season, 3B42V6 and 3B42V7 products significantly underestimated the precipitation (46.26% and 47.70% on pixel and basins scales, respectively, by 3B42V6; 20.35% and 25.20% on pixel and basin scales, respectively, by 3B42V7), while precipitation magnitudes were overestimated by 3B42RT (59.05% and 50.52% on pixel and basin scales, respectively). Figure 6 shows the patterns of evaluation indices during westerlies and monsoon months for 3B42V6, 3B42V7 and 3B42RT on pixel and basin scales. On the pixel scale, the values of r were low during both seasons. During westerlies, the values of r were 0.19, 0.32 and 0.19 for 3B42V6, 3B42V7 and 3B42RT, respectively, with the respective best values of 0.56, 0.58 and 0.42 in January (Figure 6). Meanwhile, in monsoon season the values of r were −0.01, 0.34 and 0.47 for 3B42V6, 3B42V7 and 3B42RT, respectively, with the best value of 0.31 in September for 3B42V6, 0.61 in August for 3B42V7 and 0.54 in August for 3B42RT (Figure 6). The scores of NRMSE were high in westerlies (116.94%, 107.90% and 161.97% for 3B42V6, 3B42V7 and 3B42RT, respectively) as compared with those in monsoon (59.36%, 43.04% and 98.63% for 3B42V6, 3B42V7 and 3B42RT, respectively). The NMSE showed a similar pattern as that of NRMSE with significant discrepancies in westerlies (88.17%, 81.40% and 104.66% for 3B42V6, 3B42V7 and 3B42RT, respectively) and monsoon (48.31%, 35.18% and 83.03% for 3b42V6, 3B42V7 and 3B42RT, respectively).

On the basin scale, the agreements between the gauge and TMPA-based precipitation estimates were improved in both seasons, witnessed by relatively good correlation coefficients (r = 0.43, 0.50 and 0.28 for 3B42V6, 3B42V7 and 3B42RT, respectively, in westerlies with respective best values of 0.59, 0.70 and 0.64 in January (Figure 6); r = 0.29, 0.48 and 0.36 for 3B42V6, 3B42V7 and 3B42RT, respectively, in monsoon with best value of 0.60 in September for 3B42V6, 0.79 in August for 3B42V7 and 0.54 in August for 3B42RT (Figure 6). The discrepancies showed by other indices (NRMSE = 58.24%, 103.79% and 134.23% for westerlies and respective scores of NRMSE for monsoon were 54.85%, 41.40% and 95.53%; NMAE = 46.13%, 17.93% and 104.20% for westerlies and 47.77%, 34.81% and 80.13% for monsoon for 3B42V6, 3B42V7 and 3B42RT, respectively) were lower than those on the pixel scale.

Results of the seasonal analysis revealed that, even though the performances of TMPA products were moderate during westerlies and monsoon seasons on basin scale, their agreements with the rain gauge observations in both seasons were still very poor. Therefore, TMPA products are unreliable for use in hydro-meteorological related applications during westerlies and monsoon seasons. The worse agreements between the two datasets (TMPA and gauge-based) were found in monsoon season on both pixel and basin scales. Recently, Anjum et al. [15], Chen et al. [16], and Derin et al. [20] have also reported significant over and underestimations of observed seasonal precipitation by real and post real time TMPA products in different regions of the world.

In summary, despite the fact that the accuracy of the new version (3B42V7) of TMPA products was low (better than 3B42V6 and 3B42RT) on daily scale, its performance was moderate on monthly and annual scales with slight underestimation (−6.24%). Moreover, the evaluation results suggest that the performance of satellite-based precipitation products increased with increasing spatial scale. The BIAS in 3B42V7 has been improved by 85.90% and 116.16% compared with 3B42V6 and 3B42RT, respectively.

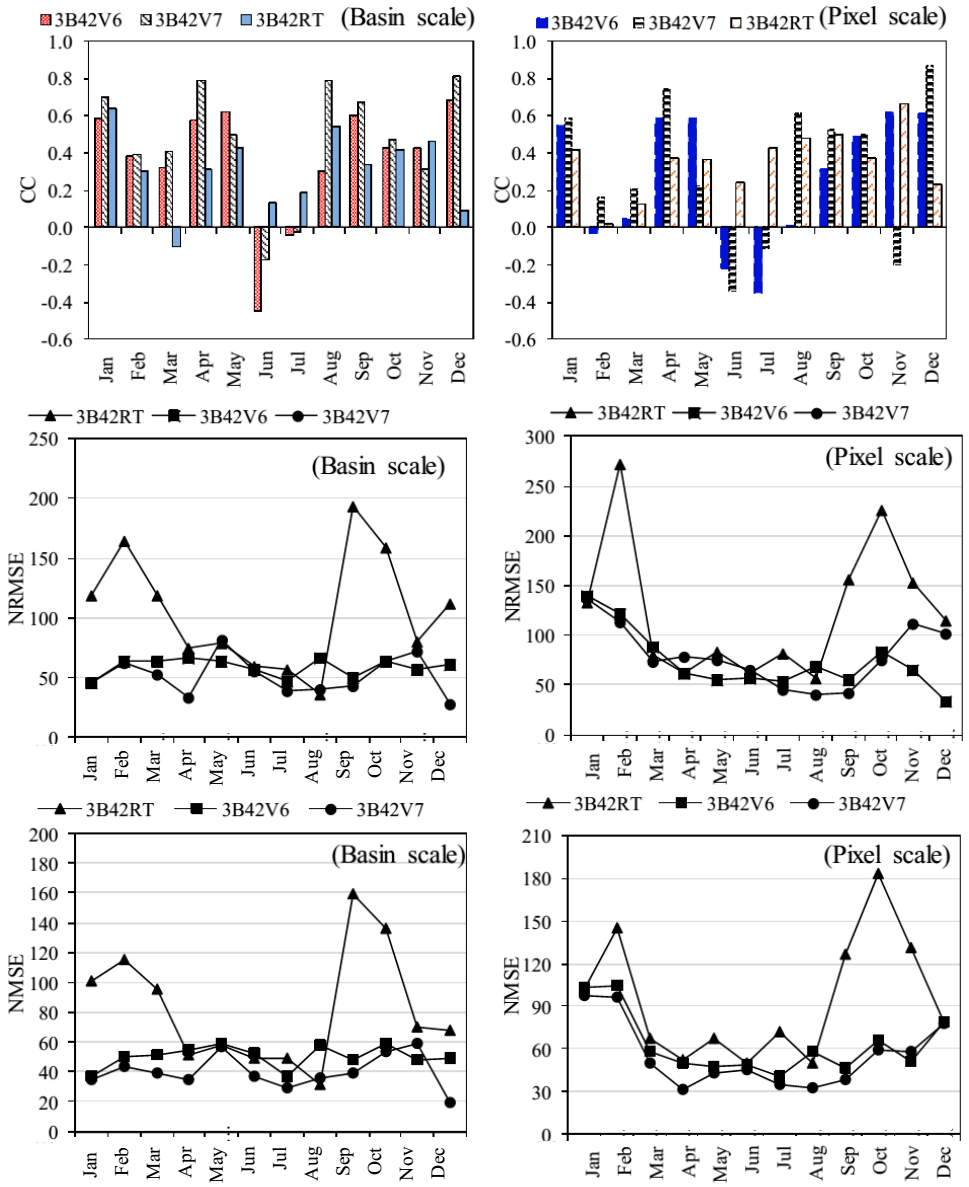

Figure 6. Mean monthly statistical indices (CC, NRMSE and NMSE) on pixel and basin scales.

3.3. Accuracy of TMPA Products at Different Precipitation Intensities

The ability of TMPA products to detect the occurrence of precipitation at different intensities was evaluated. Evaluation results show that precipitation detection capability of the TMPA products decreases with the increase in precipitation intensity (Figure 7). Overall abilities of 3B42V6, 3B42RT and 3B42V7 to detect the precipitation intensities more than 1 mm/day were less than 40% (Figure 7a,d,g). Among all TMPA products, 3B42RT showed the minimum POD. POD of all TMPA products showed a decreasing trend with the increase in precipitation intensities. It revealed that the accuracy of TMPA products to detect the intense precipitation events was very low. Analysis of FAR showed that the ratio of estimation of false precipitation events was increased with the increase of precipitation intensities (Figure 7b,e,h). FAR scores for 3B42RT were higher than those of 3B42V6 and 3B42V7. Similarly, the agreement between TMPA products and gauge based observations decreased with the increase in precipitation intensities (Figure 7c,f,i). The scores of CSI for 3B42V7 were better than those of 3B42V6 and 3B42RT. Estimation of errors and relative errors (Figure 8) revealed that 3B42V6 underestimated the light and moderate precipitation intensities (0–9 mm/day) and overestimated the

heavy precipitation rates (>9 mm/day) (Figure 8a). For 9–12 mm/day, the overestimation was 82.9%. On the other hand, very light precipitation intensities (0–≤ 0.5 mm/day) were slightly overestimated (4.2%) and the light precipitation intensities from >0.5–3 mm/day were underestimated (43.7%) by 3B42V7. More significant underestimations by 3B42V7 were found for moderate to high precipitation intensities (>3 mm/day) (Figure 8b). Very light precipitation intensities (<3 mm/day) were underestimated by 3B42RT and precipitation intensities more than 3 mm/day were overestimated by this product (Figure 8c). These results revealed that the TMPA products were less skillful to detect the magnitude and occurrence of intense precipitation events, which is consistent with the findings in the Hindukush Mountains [15]. The reason behind poor performance of TMPA products while capturing the precipitation events was, probably the cryospheric climate, complex topography and orographic lifting in the high mountains. In IR based precipitation algorithms, cloud top temperature threshold values were used to estimate the precipitation but that temperature was too low in case of orographic clouds which ultimately leads to a higher error in detection of precipitation occurrence. Furthermore, ice aloft in the high mountains causes scattering of passive microwaves (PW) which eventually results an error in the estimation of precipitation magnitude. Therefore, high error in estimation of precipitation in this region is because of the IR and PM based algorithms used in the TMPA-based precipitation retrievals.

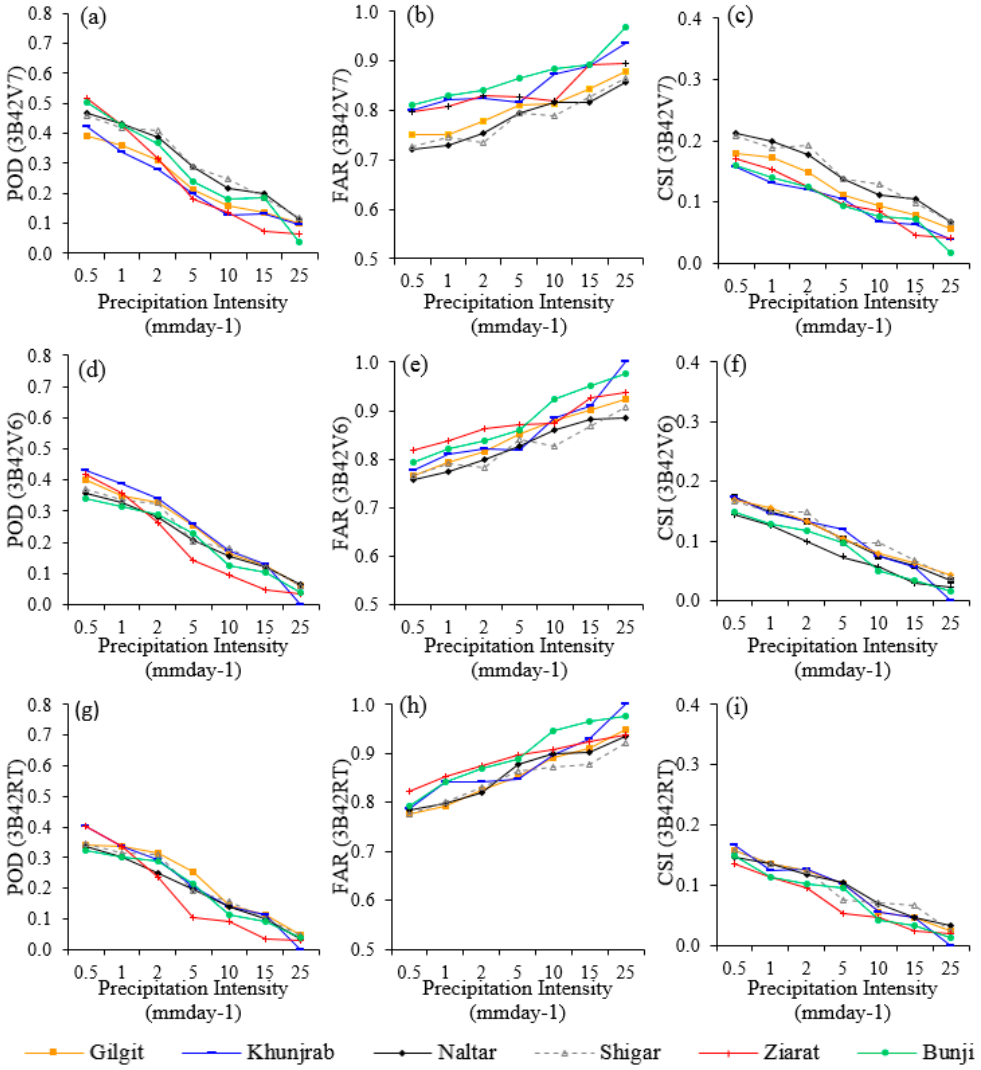

Figure 7. Categorical statistics of: 3B42V7 (**a**–**c**); 3B42V6 (**d**–**f**); and 3B42RT (**g**–**i**) for probability of detection (POD), false alarm ratio (FAR), and critical success index (CSI).

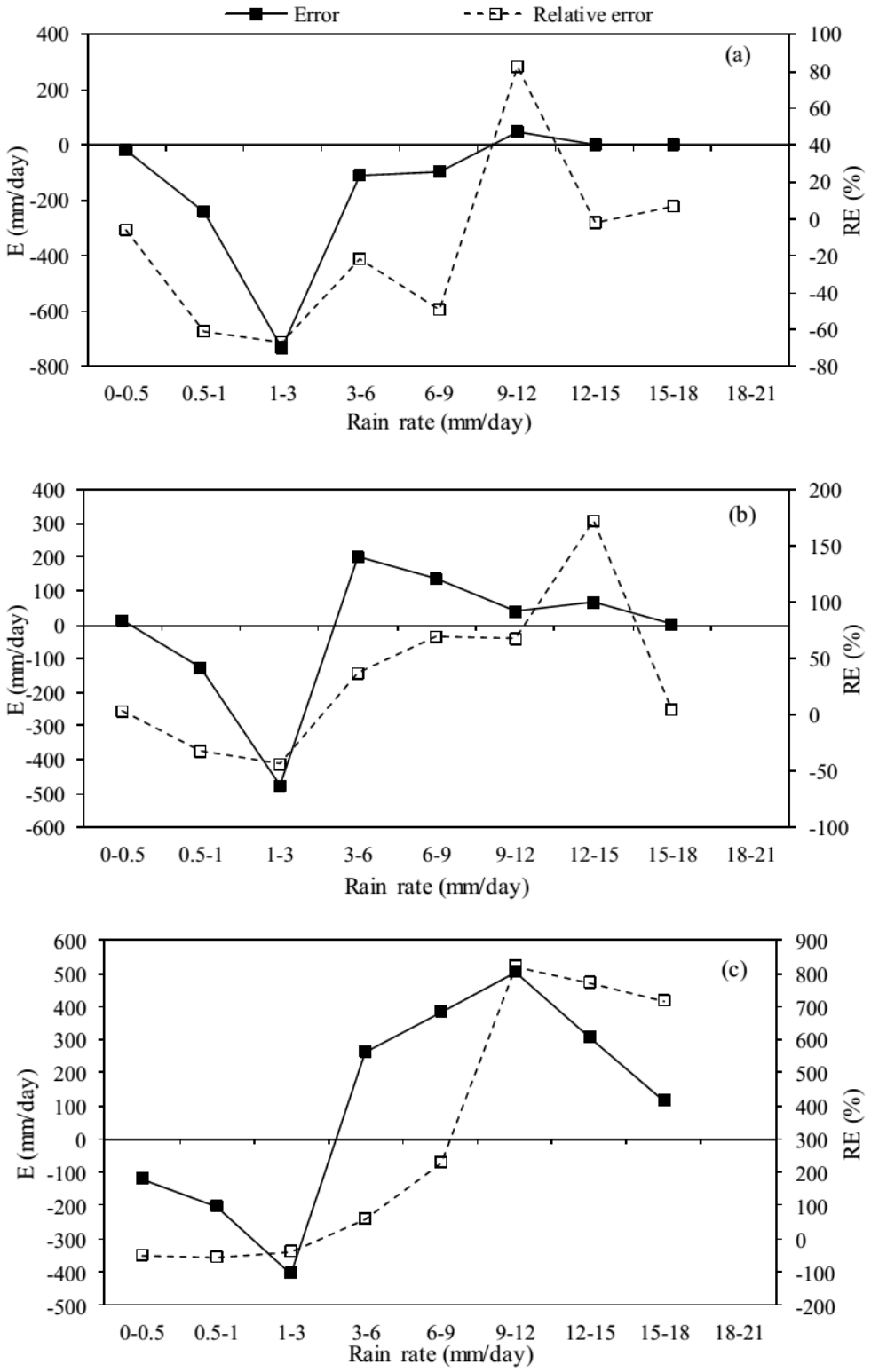

Figure 8. The precipitation differences and relative errors at different precipitation intensities for: (**a**) 3B42V6; (**b**) 3B42V7; and (**c**) 3B42RT.

Overall, the performance of the precipitation estimates derived from gauge adjusted 3B42V7 product were better than that of its predecessor bias adjusted 3B42V6 and unadjusted 3B42RT products in the northern Pakistan. Compared to the 3B42V6 and 3B42RT, the 3B42V7 exhibited improvements in Bias, CC, RMSE, POD, FAR and CSI at all time periods, which was consistent with the findings in

Bhutan [33], India [10], Morocco [13], and China [28]. Despite the fact that 3B42V7 showed superiorities over 3B42V6 and 3B42RT, it still exhibits poor agreements with the gauge-based reference data at daily and seasonal time scales as analyzed with lower values of CC. To date, the daily and seasonal precipitation estimates derived from 3B42V7 were found to have poor correlation with the reference data in Hindukush Mountainous range [15,19], Tanzania [9], Malaysia [34], Taiwan, the U.S. Rocky Mountains and Nepal [20]. In contrast, a good correlation was found in China [28], Turkey [20], and Morocco [13]. A good correlation in these regions may be because more gauging stations were used in bias correction algorithm of TMPA products [5]. Selection of the limited number of reference ground-based gauging station in the bias correction algorithms of TMPA products could be one of the potential reasons behind poor correlations of TMPA products with reference gauges data in the northern Pakistan. To adequately enhance the reliability of satellite-based precipitation estimates, more ground-based reference gauging stations from the complex terrain regions, such as northern Pakistan, should be incorporated in bias correction algorithms of satellite-based precipitation products.

4. Conclusions

Increase in population has multiplied the demand of available water for food security, hydropower projects, ecological use and anthropogenic water use. It signifies the need of better understanding of quality and quantity of water resources to ascertain the sustainable water supplies. The rain gauge stations in the Hunza River basins situated in northern Pakistan are very few and sparse. Satellite precipitation estimates are being utilized broadly as an alternative of rain gauge observations for physically inaccessible mountain ranges. However, robust quality evaluation is necessary before the direct utilization of these products for different hydro-meteorological applications. This study was conducted to evaluate the performance of three TMPA-based precipitation products (3B42V6, 3B42RT and 3B42V7) in estimating daily, monthly, seasonal and annual precipitation on different spatial (pixel and basin) scales over Hunza River basin, northern Pakistan using in-situ rain gauge data. The findings of this study revealed the following conclusions:

(1) The 3B42V6 and 3B42RT products failed to capture the spatial pattern of observed precipitation over the Hunza Basin, while 3B42V7 adequately followed the spatial pattern of observed precipitation over the Hunza Basin.

(2) The performances of TMPA products were very poor in daily precipitation estimations on both spatial (pixel and basin) scales. The agreements between the daily gauge-based precipitation and TMPA-based estimates were low ($r < 0.50$, on both pixel and basin scales). They also failed to estimate the precipitation magnitudes. The 3B42V6 significantly underestimated the precipitation magnitudes on both spatial pixel (−31.25%) and basin (44.27%) scales, while 3B42V7 overestimated the precipitation on pixel scale (17.31%) but slightly underestimated on basin scale (6.24%). On the other hand, 3B42RT overestimated the precipitation on both pixel (47.9%) and basin (38.6%) scales. Although the performances improved with increasing spatial scale, all TMPA products were found unreliable on the daily scale because of high errors in Karakoram Region.

(3) All TMPA products showed poor performances in westerlies and monsoon seasons. In westerlies, 3B42V6 and 3B42V7 significantly underestimated the precipitation on both basin and pixel scales (>45% and >20%, respectively). In both rainy seasons, the r of all TMPA products with the rain gauge observations was low (<0.50) and errors were high. Thus, westerlies and monsoon TMPA-based precipitation estimates are not suitable for direct applications in Karakoram Region.

(4) On the monthly and annual scales, 3B42V6 and 3B42RT were unreliable on both pixel and basin scales, with low r values (with the highest value of $r = 0.52$ for 3B42V6 on monthly scale and 0.46 for 3B42RT on the annual scale) and significant BIAS (>30%). However, 3B42V7 showed good agreements with gauge observations on the basin scale as exhibited by high r vales ($r > 0.60$ and > 0.70 on monthly and annual scales, respectively) and low BIAS (−6.24%).

(5) The TMPA products are unreliable to capture the intense precipitation events in the studied region. POD and CSI scores decreased with the increase in precipitation intensities, while FAR increased with the increase of thresholds. Therefore, TMPA products are not suitable for modeling, monitoring, and forecasting of floods in Karakoram Region.

(6) The overall performance of new version (3B42V7) of TMPA products was better than 3B42V6 and 3B42RT (85.90% BIAS was improved as compared to 3B42V6 and 116.16% as compared to 3B42RT).

Findings of this study suggest that 3B42V7 product is reliable for hydrological and related applications on the monthly and annual scales with careful calibration. The poor performances of TMPA products on daily and seasonal scales emphasize the need to improve the TMPA-based precipitation algorithms. We recommend that regional bias correction of TMPA products should be conducted on daily and seasonal timescales for getting reliable precipitation substitutes before utilizing them for any research and operational work in future. Therefore, the future study would focus on the establishment of regional bias correction algorithms and utilization of bias-corrected satellite precipitation estimates in hydrological modeling. Findings of this study would be useful for researchers, water resources managers as well as for algorithm developers of TMPA and Global Precipitation Measuring (GPM) Mission (an extension of TRMM) to provide better spatio-temporal coverage of global precipitation with more advanced dual frequency radar on board.

Acknowledgments: This study was supported by the Ministry of Science and Technology of China (Grant: 2013CBA01804) and the National Natural Science Foundation of China (Grant: 41425003 and 41671058). The authors are grateful to the WAPDA and PMD for providing the data.

Author Contributions: Cunde Xiao supervised and developed the research framework; Ayaz Fateh Ali and Muhammad Naveed Anjum processed and analysed the data, outlined the finding and wrote the manuscript; Muhammad Adnan and Zain Nawaz contributed to design the manuscript; Muhammad Wajid Ijaz contributed to analyse the data and review of the manuscript; Muhammad Sajid and Hafiz Umar Farid contributed in data collection, writing and review of the manuscript. Overall this article is great deal of coordinated effort.

Conflicts of Interest: The authors declare no conflict of interest.

Appendix A

Formulas of continuous evaluation indices are as follows:

The linear regression is given by:

$$y_e = ax_o + b \tag{A1}$$

where x_o is the observed (gauge-based) precipitation; y_e estimated (satellite-based) precipitation; and a and b are the linear regression coefficients. Value of a close to one represents the high level of consistency between the satellite and gauge precipitation data.

The Pearson's correlation coefficient (r) can be described as following:

$$r = \frac{\sum_{i=1}^{n}(G_i - G)(S_i - S)}{\sqrt{\sum_{i=1}^{n}(G_i - G)^2} \times \sqrt{\sum_{i=1}^{n}(S_i - S)^2}} \tag{A2}$$

where n denotes the total satellite and gauge data pairs; G_i and S_i are the gauge and satellite precipitation data, respectively; and G and S are average values of gauge and satellite precipitation data.

The formulas of these indices are given by:

$$E = Si - Gi \tag{A3}$$

$$RE = \frac{S_i - G_i}{G_i} \times 100 \tag{A4}$$

$$ME = \frac{1}{n}\sum_{i=1}^{n}(S_i - G_i) \tag{A5}$$

$$MAE = \frac{1}{n}\sum_{i=1}^{n}|S_i - G_i| \tag{A6}$$

$$NMAE = \frac{MAE}{G} \times 100 \tag{A7}$$

$$BIAS = \frac{\sum_{i=1}^{n}(S_i - G_i)}{\sum_{i=1}^{n} G_i} \times 100 \tag{A8}$$

$$RMSE = \sqrt{\frac{1}{n}\sum_{i=1}^{n}(S_i - G_i)^2} \tag{A9}$$

$$NRMSE = \frac{RMSE}{G} \times 100 \tag{A10}$$

Formulas of categorical indices are as follows:

$$POD = \frac{H}{H + M} \tag{A11}$$

$$FAR = \frac{F}{H + F} \tag{A12}$$

$$CSI = \frac{H}{H + M + F} \tag{A13}$$

where F represents the precipitation detected by satellite when there is no actual precipitation occurrence; H represents the precipitation observed by gauge and correctly detected by satellite; and M represents the precipitation observed by gauge but not detected by satellite.

References

1. Munoz, E.A.; Di Paola, F.; Lanfri, M. Advances on Rain Rate Retrieval from Satellite Platforms using Artificial Neural Networks. *IEEE Latin Am. Trans.* **2015**, *13*, 3179–3186.
2. Huffman, G.J.; Adler, R.F.; Curtis, S.; Bolvin, D.T.; Nelkin, E.J. Global rainfall analyses at monthly and 3-h time scales. Measuring Precipitation from Space: EURAINSAT and the Future. *Adv. Glob. Chang. Res.* **2007**, *28*, 291–305.
3. Casella, D.; Dietrich, S.; Di Paola, F.; Formenton, M.; Mugnai, A.; Porcù, F.; Sanò, P. PM-GCD—A combined IR–MW satellite technique for frequent retrieval of heavy precipitation. *Nat. Hazards Earth Syst. Sci.* **2012**, *12*, 231–240.
4. Huffman, G.J.; Bolvin, D.T.; Nelkin, E.J.; Adler, R.F. The TRMM multisatellite precipitation analysis (TMPA): Quasi-global, multiyear, combined-sensor precipitation estimates at fine scales. *J. Hydrometeorol.* **2007**, *8*, 38–55.
5. Tan, M.L.; Duan, Z. Assessment of GPM and TRMM Precipitation Products over Singapore. *Remote Sens.* **2017**, *9*, 720. [CrossRef]
6. Stisen, S.; Sandholt, I. Evaluation of remote-sensing-based rainfall products through predictive capability in hydrological runoff modelling. *Hydrol. Process.* **2010**, *24*, 879–891.
7. Arias-Hidalgo, M.; Bhattacharya, B.; Mynett, A.E.; Van Griensven, A. Experiences in using the TMPA-3B42R satellite data to complement rain gauge measurements in the Ecuadorian coastal foothills. *Hydrol. Earth Syst. Sci.* **2013**, *17*, 2905–2915. [CrossRef]
8. Chen, S.; Hong, Y.; Cao, Q.; Gourley, J.J.; Kirstetter, P.-E.; Yong, B.; Tian, Y.; Zhang, Z.; Shen, Y.; Hu, J.; et al. Similarity and difference of the two successive V6 and V7 TRMM multisatellite precipitation analysis performance over China. *J. Geophys. Res. Atmos.* **2013**, *118*, 13060–13074. [CrossRef]
9. Mashingia, F.; Mtalo, F.; Bruen, M. Validation of remotely sensed rainfall over major climatic regions in Northeast Tanzania. *Phys. Chem. Earth Parts A/B/C* **2014**, *67*, 55–63. [CrossRef]
10. Prakash, S.; Mitra, A.K.; Momin, I.M.; Pai, D.S.; Rajagopal, E.N.; Basu, S. Comparison of TMPA-3B42 versions 6 and 7 precipitation products with gauge-based data over India for the southwest monsoon period. *J. Hydrometeorol.* **2015**, *16*, 346–362. [CrossRef]

11. Mishra, A.; Gairola, R.M.; Varma, A.K.; Agarwal, V.K. Remote sensing of precipitation over Indian land and oceanic regions by synergistic use of multisatellite sensors. *J. Geophys. Res. Atmos.* **2010**, *115*, 462–474. [CrossRef]
12. Bitew, M.M.; Gebremichael, M.; Ghebremichael, L.T.; Bayissa, Y.A. Evaluation of high-resolution satellite rainfall products through streamflow simulation in a hydrological modeling of a small mountainous watershed in Ethiopia. *J. Hydrometeorol.* **2012**, *13*, 338–350. [CrossRef]
13. Jamandre, C.; Narisma, G. Spatio-temporal validation of satellite-based rainfall estimates in the Philippines. *Atmos. Res.* **2013**, *122*, 599–608. [CrossRef]
14. Milewski, A.; Elkadiri, R.; Durham, M. Assessment and comparison of TMPA satellite precipitation products in varying climatic and topographic regimes in Morocco. *Remote Sens.* **2015**, *7*, 5697–5717. [CrossRef]
15. Anjum, M.N.; Ding, Y.; Shangguan, D.; Tahir, A.A.; Iqbal, M.; Adnan, M. Comparison of two successive versions 6 and 7 of TMPA satellite precipitation products with rain gauge data over Swat Watershed, Hindukush Mountains, Pakistan. *Atmos. Sci. Lett.* **2016**, *17*, 270–279. [CrossRef]
16. Chen, S.; Hong, Y.; Gourley, J.J.; Huffman, G.J.; Tian, Y.; Cao, Q.; Yong, B.; Kirstetter, P.-E.; Hu, J.; Hardy, J.; et al. Evaluation of the successive V6 and V7 TRMM multisatellite precipitation analysis over the Continental United States. *Water Resour. Res.* **2013**, *49*, 8174–8186. [CrossRef]
17. Khan, S.I.; Hong, Y.; Gourley, J.J.; KhanKhattak, M.U.; Yong, B.; Vergara, H.J. Evaluation of three high-resolution satellite precipitation estimates: Potential for monsoon monitoring over Pakistan. *Adv. Space Res.* **2014**, *54*, 670–684. [CrossRef]
18. Liu, Z. Comparison of precipitation estimates between Version 7 3-hourly TRMM Multi-Satellite Precipitation Analysis (TMPA) near-real-time and research products. *Atmos. Res.* **2015**, *153*, 119–133. [CrossRef]
19. Anjum, M.N.; Ding, Y.; Shangguan, D.; Ijaz, M.W.; Zhang, S. Evaluation of High-Resolution Satellite-Based Real-Time and Post-Real-Time Precipitation Estimates during 2010 Extreme Flood Event in Swat River Basin, Hindukush Region. *Adv. Meteorol.* **2016**. [CrossRef]
20. Derin, Y.; Anagnostou, E.; Berne, A.; Borga, M.; Boudevillain, B.; Buytaert, W.; Chang, C.-H.; Delrieu, G.; Hong, Y.; Hsu, Y.C.; et al. Multiregional Satellite Precipitation Products Evaluation over Complex Terrain. *J. Hydrometeorol.* **2016**, *17*, 1817–1836. [CrossRef]
21. Cimini, D.; Romano, F.; Ricciardelli, E.; Di Paola, F.; Viggiano, M.; Marzano, F.S.; Colaiuda, V.; Picciotti, E.; Vulpiani, G.; Cuomo, V. Validation of satellite OPEMW precipitation product with ground-based weather radar and rain gauge networks. *Atmos. Meas. Tech.* **2013**, *6*, 3181–3196. [CrossRef]
22. Zhang, Q.; Liu, Y.; Yang, G.; Zhang, Z. Precipitation and hydrological variations and related associations with large-scale circulation in the Poyang Lake basin, China. *Hydrol. Process.* **2011**, *25*, 740–751. [CrossRef]
23. Liu, Y.; Wu, G.; Zhao, X. Recent declines in China's largest freshwater lake: Trend or regime shift? *Environ. Res. Lett.* **2013**, *8*, 14010–14019. [CrossRef]
24. Guo, R.; Liu, Y. Evaluation of Satellite Precipitation Products with Rain Gauge Data at Different Scales: Implications for Hydrological Applications. *Water* **2016**, *8*, 281. [CrossRef]
25. Chevallier, P.; Arnaud, Y.; Ahmad, B. Snow cover dynamics and hydrological regime of the Hunza River basin, Karakoram Range, northern Pakistan. *Hydrol. Earth Syst. Sci.* **2011**, *15*, 2259–2274.
26. World Meteorological Organization. *Guide to Hydrological Practices: Data Acquisition, and Processing, Analysis, Forecasting and Other Applications*; World Meteorological Organization: Geneva, Switzerland, 1994.
27. Huffman, G.J.; Adler, R.F.; Bolvin, D.T.; Nelkin, E.J. *The TRMM Multi-Satellite Precipitation Analysis (TMPA), in Satellite Rainfall Applications for Surface Hydrology*; Springer: Dordrecht, The Netherlands, 2010; pp. 3–22.
28. Zhao, Y.; Xie, Q.; Lu, Y.; Hu, B. Hydrologic Evaluation of TRMM Multisatellite Precipitation Analysis for Nanliu River Basin in Humid Southwestern China. *Nat. Sci. Rep.* **2017**, *7*, 2470. [CrossRef] [PubMed]
29. Denis, M. Cokriging With Matlab. *Comput. Geosci.* **1991**, *17*, 1265–1280.
30. Adhikary, S.K.; Muttil, N.; Yilmaz, A.G. Cokriging for enhanced spatial interpolation of rainfall in two Australian catchments. *Hydrol. Process.* **2017**, *31*, 2143–2161. [CrossRef]
31. Romilly, T.G.; Gebremichael, M. Evaluation of satellite rainfall estimates over ethiopian river basins. *Hydrol. Earth Syst. Sci.* **2011**, *15*, 1505–1514. [CrossRef]
32. Prakash, S.; Sathiyamoorthy, V.; Mahesh, C.; Gairola, R.M. An evaluation of high-resolution multisatellite rainfall products over the Indian monsoon region. *Int. J. Remote Sens.* **2014**, *35*, 3018–3035. [CrossRef]

33. Xue, X.; Hong, Y.; Limaye, A.S.; Gourley, J.J.; Huffman, G.J.; Khan, S.I.; Dorji, C.; Chen, S. Statistical and hydrological evaluation of TRMM-based Multi-satellite Precipitation Analysis over the Wangchu Basin of Bhutan: Are the latest satellite precipitation products 3B42V7 ready for use in ungauged basins? *J. Hydrol.* **2013**, *499*, 91–99. [CrossRef]
34. Tan, M.T.; Ibrahim, A.; Duan, Z.; Cracknell, A.; Chaplot, V. Evaluation of Six High-Resolution Satellite and Ground-Based Precipitation Products over Malaysia. *Remote Sens.* **2015**, *7*, 1504–1528. [CrossRef]